WAVELET ENHANCEMENT OF CLOUD-RELATED SHADOW AREAS IN SINGLE LANDSAT SATELLITE IMAGERY

A. Abd-Elrahman[a], M. Elhabiby[b]

[a] School of Forest Resources and Conservation – Geomatics, University of Florida – aamr@ufl.edu
[b] Department of Geomatics Engineering, University of Calgary - mmelhabi@ucalgary.ca

Commission VII, WG VII/6

KEY WORDS: Wavelet, image fusion, shadow, frequency decomposition, Landsat

ABSTRACT:

Cloud-related shadows represent areas with low illumination conditions that affect remote sensing image quality. In this research, a wavelet-based image sharpening algorithm was developed to enhance shadow areas independently using the defected cloudy image information. The developed algorithm is applied locally by boosting the image high frequency content in the shadow areas using the defected image de-noised wavelet coefficients. Image entropy was used as a measure to determine the change in wavelet coefficient values. The developed algorithm was tested on the panchromatic band of a November 2001 Landsat 7 ETM satellite subscenes. Another cloud-free image was used as reference image for results evaluation and quality analysis. Several discrete wavelet decomposition levels were tested. Quantitative measures were used to evaluate the obtained results. Visual and quantitative analysis of the results revealed that the ability to enhance details under shadow areas increased with the increase in the number of wavelet decomposition levels. Two or three wavelet decomposition levels were found to be sufficient for enhancing image quality in the shadow areas while avoiding introduced artifacts. Conclusions and recommendations are given with respect to the suitability, accuracy and efficiency of this method.

1. INTRODUCTION

Small cloud patches are very common in the images taken in many parts of the world. This problem of clouds and cloud-associated shadows are widely spread with approximately 66% of the earth surface is covered by clouds throughout the year (Belward and Valenzuela,1991). Although these cloud areas can easily be detected due to their high reflectance, the shadows caused by these clouds represent areas with low illumination conditions that are harder to detect but have the potential for enhancement. Cloud-related shadow removal is normally handled by first detecting the cloud and shadow areas. Then, image intensities in the shadow regions are adjusted to enhance the image quality. Different methodologies are developed and implemented for shadow detection that utilizes geometric constraints in addition to the image spectral characteristics (Abdelwahab,2006; Simpson and Stitt,1998).

Some of these methods identifies and removes the image illumination variations using surface reflectance and variations constraints (Finlayson et al.,2002; Marini and Rizzi,2000). Such methods were implemented mostly on high spatial resolution imagery and suffer costly computational overhead in addition to shadow edge processing problems. Other methods utilized overlapping imagery to detect occlusion and remove shadows (Zhou et al.,2003). Fusion techniques were also used to account for cloud and shadow defects on certain image using different cloud/shadow free images (Berbar and Gaber,2004; Wang and Ono,1999). Although these methods are widely used, they require another cloud free image taken at different time to compensate for defects in the cloud and shadow regions. Temporal image variations represent a major source of error in the output enhanced image.

Shadow restoration from a single image can be looked at as an intensity adjustment process. Simply adjusting the brightness and contrast of the image cannot remove the shadow effect. The fact that shadows smooth brightness variations reduces the shadow removal process to an image sharpening process applied locally to the shadow area. Image sharpening can be done in the spatial or frequency domains (Haralick and Shapiro,1992). One of the methods used in the frequency domain is the wavelet. The frequency domain provides the flexibility to model frequency content differently at each wavelet decomposition level. Wavelet analysis was used for image sharpening in applications that range from mammogram image sharpening (Bouyahia et al.,2004) to enhancement of scanned images (Barkener,2002).

In this research, wavelet sharpening will be used to boost the high frequency content in shadow areas. Only the cloudy image will be used for such analysis. In the following sections, the methodology implemented in this research will be described followed by a numerical example. Experiment results, analysis and final conclusions are then presented.

2. BACKGROUND AND METHODOLOGY

2.1 Discrete Wavelet Transform

Wavelet decomposition and reconstruction was extensively used in image fusion and compression applications. Discrete wavelet transform will be utilized in this research paper to enhance cloud-related shadow areas by adjusting their frequency content.

Let $\phi_{jk} = \phi(2^j x - k)$ and $\psi_{jk} = \psi(2^j x - k)$ be sets of dilated scaled and wavelet functions, respectively. Both functions can be constructed from the higher level scaling functions (Burrus,1998):

$$\phi(2^{j-1}x) = \sum_k h_{j+1}(k)\phi(2^j x - k) \quad (1)$$

$$\psi(2^{j-1}x) = \sum_k g_{j+1}(k)\phi(2^j x - k) \quad (2)$$

Where *h(k)* and *g(k)* are low and high pass filters respectively. Any function *f(x)* can be represented by given scaling and wavelet coefficients with respect to the corresponding functions as:

$$f(x) = \sum_k c_{j-1_0}(k)\phi(2^{j-1}x - k) + \sum_k d_{j-1}(k)\psi_{j,k}(2^{j-1}x - k) \quad (3)$$

For orthonormal scaling and wavelet functions the scaling (approximation) and wavelet (detail) coefficients can be represented in terms of their values in a previous scale as follows:

$$c_{j-1}(k) = \sum_m h(m-2k)c_j(m) \quad (4)$$

$$d_{j-1}(k) = \sum_m g(m-2k)d_j(m) \quad (5)$$

Recalling that the scaling function application on the signal is a low pass filter and the wavelet function application on the signal is a high pass filter, it can be concluded that obtaining the approximation and detail coefficient constitutes a single step in an iterative filter bank that results in multiple level decomposition of the signal. This iterative filter bank forms the basis of the discrete wavelet transform. A reverse operation can also be used to completely reconstruct the signal. In image analysis, a generalized form of the one-dimensional discrete wavelet transform can be used, by applying tensor product between the two sets of coefficients in the *x* and *y* directions. A scaling and wavelet transform can be defined as follows:

$\Phi(x, y) = \phi(x)\,\phi(y)$ (6)

$\Psi 1(x, y) = \phi(x)\,\psi(y)$ (7)

$\Psi 2(x, y) = \psi(x)\,\phi(y)$ (8)

$\Psi 3(x, y) = \psi(x)\,\psi(y)$ (9)

Where *Φ(x, y), Ψ1(x, y), Ψ2(x, y), and Ψ3(x, y)* are the scaling, vertical, horizontal, and vertical wavelet functions, respectively.

2.2 Quality Analysis)

Another cloud free image of the area could be used as a base for assessing the quality of the developed algorithm. Two metrics suggested in this analysis, which are the root mean square error (RMSE) and the entropy. The RMSE can be expressed as follows:

$$RMSE = \sqrt{Ex(\left|(u(m,n) - v(m,n)\right|^2)}$$

Where *u(m,n)* and *v(n,m)* represent the tested and reference images respectively. The increase in the RMSE value indicates more differences between the tested and the reference images. The second metric is the image entropy, which represent the amount of information in the image and can be expressed as follows:

$$Ent = \sum_i p(d_i)\log_2 p(d_i)$$

where d_i is the number of gray levels possible and $p(d_i)$ is the probability of occurrence of a particular gray level.

2.3 Developed Algorithm

Modification of the wavelet detail coefficients is an efficient way to perform an adaptive image enhancement. A schematic diagram of the developed algorithm for image enhancement in shadow areas, which depends on enhancing the image details content, is shown in Figure 1.

A contrast shift is applied to the image so that the gray values in the shadow areas have the same range as the rest of the image.

1. The Biorthogonal wavelet family (Biro2,2) is used due to its linear phase property. The image is decomposed into multiple levels using the Bior2,2 discrete wavelet transform. The resulting approximation and detail coefficients are denoted c_j and d_j respectively, where *j* refers to the wavelet decomposition level. It should be noted here that the detail coefficient d_j refer to the horizontal, vertical, and diagonal coefficients mentioned in Equations 7, 8, and 9. The universal threshold is used with fixed values in all wavelets levels and directions (vertical,

horizontal and diagonal) and the threshed value is computed as follows:

$T_{univ} = \sigma_n\sqrt{2log(n)}$ Where σ_n is the estimate of the standard deviation of additive white noise and n is the total number of the wavelet coefficients in a given detail image.

2. An image denoising algorithm is applied to attenuate the image noise content. A soft thresholding (universal technique) (Donoho,1995) is applied to the image detail coefficients at each level. This step is applied to attenuate the image noise content before magnifying image details resulting in a reduced noise levels in output details coefficients d_j^{de} .

3. The original image coefficients are modified by adding a percentage of the noise-attenuated coefficient values to produce new coefficient values d_j^f . The percentage used depends on the image entropy in the shadow areas , in addition to the entropy of the rest of the image, excluding cloud areas. The new coefficient values at each level are computed using:

$$d_j^f = \alpha d_j^{de} + d_j \quad (10)$$

Where $\alpha = \dfrac{E_{image}}{E_{shadow}}$

4. The image is finally reconstructed using the original approximation and modified details c_j and d_j^f at each level.

5. In the spatial domain, a final image is produced that has original image values in the non-shadow areas and the modified image resulting from step 4 in the shadow areas. Shadow edges are then smoothed using a Gaussian operator.

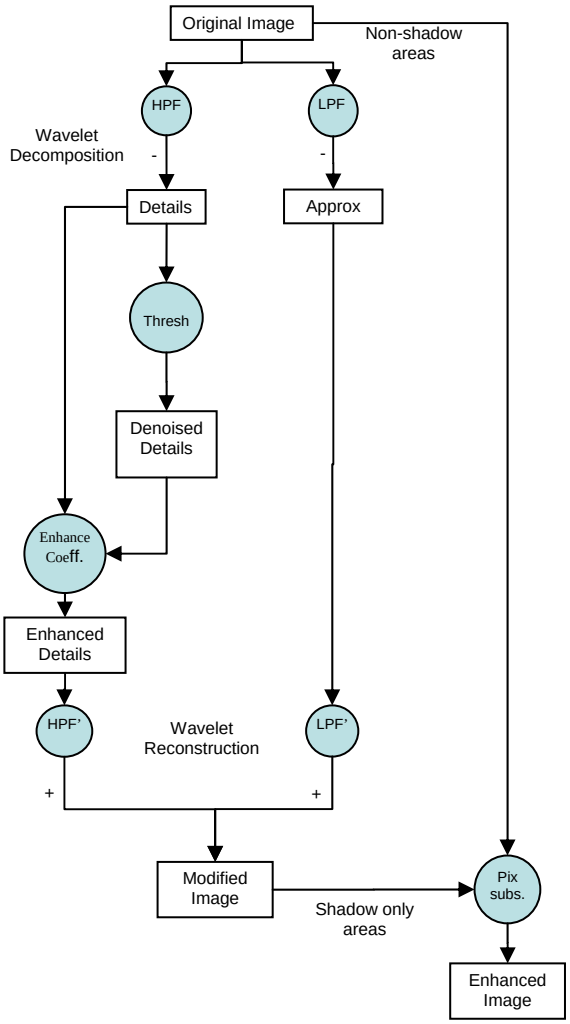

Figure 1. Schematic diagram of developed algorithm

3. EXPERIMENT

3.1 Data

The developed algorithm was implemented on the panchromatic band of a November 2001 Landsat 7 ETM satellite subscenes, shown in Figure 2. This area represents part of a city suburb located close to an airport close to Cairo, Egypt. Features in this image are partially obscured by existing cloud patches and their associated shadows. It should be mentioned that for simplicity the boundary problems were solved by allowing the application to process the original scene outside the boundaries of the test subscenes when needed, especially for shadow detection stage. Figure 3 shows parts of the study image where a runway and road intersection are partially shown in shadow areas.

Figure 2. Landsat ETM subscene with clouds and cloud-related shadows

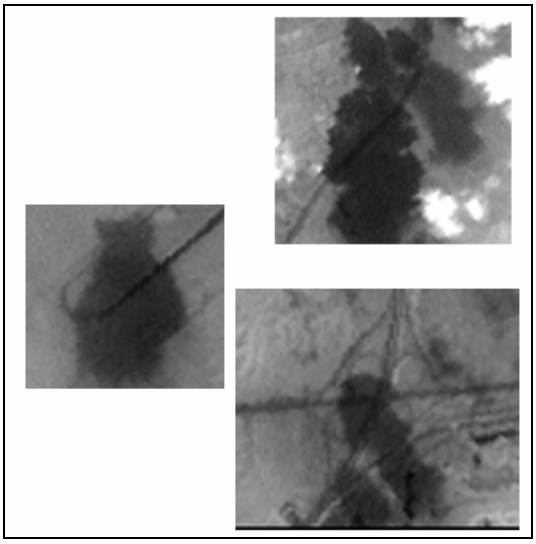

Figure 3. Features partially obscured by cloud shadows

Another cloud-free image, shown in Figure 4 was used as a reference image for the results evaluation and quality analysis. This image is another ETM Panchromatic image of the same spatial resolution taken in July 2000. The small time difference between the two images minimizes the expected temporal differences taking into consideration the arid nature of the imaged area.

Figure 4. Cloud-free images–July 2000 Landsat7 ETM panchromatic subscene

3.2 Shadow Detection

Many algorithms were developed to detect clouds and their associated shadows. Concepts such as simple thresholding (Shaker et al.,2005) and fuzzy logic (Lissens, et al.,2000) were utilized in these algorithms. The wavelet methodology applied in this research utilizes clouds-shadow geometric constraints in addition to their spectral characteristics (Abdelwahab,2006). In this methodology, clouds and shadows are first classified using neural network classification process, which mainly depends on selecting training sets and perform automatic classification based on image spectral properties. Then, the classification results are improved by defining the spatial relationship between cloud patches and their corresponding shadows.

A linear mathematical model is assumed and a least squares adjustment process is performed to estimate model parameters. The model then is used to filter out non-shadow pixels. Accuracy assessment results showed 11% and 19% commission and omission percentage errors respectively. Most of the errors were found to be at the edges of the shadow areas. It is believed that this methodology needs further enhancement to overcome the high percentage of the omission errors. However, this is considered outside the scope of this research which focuses mainly on image enhancement in the shadow areas.

3.3 Image Enhancement using Developed Algorithm

A histogram shift is applied to the shadow areas in the tested image. The shift value is extracted from the difference between the median gray level value in the shadow regions and the corresponding median in the rest of the image, excluding the identified cloud regions. This modification increases the gray level values in the shadow areas to approach those in the shadow/cloud free areas. The modified image is then decomposed using one of the Biorthogonal wavelet families Bior(2,2). One to four levels of decomposition were tested.

A universal threshold denoising algorithm, introduced in section 2.3, was applied to attenuate noise in the mage based on Dononho,(1992). In this technique, high magnitude detail

wavelet coefficients are considered noise and filtered out. The original image coefficients are then modified by adding a percentage of the corresponding denoised coefficient. This percentage was determined based on the percentage of image entropy in the image excluding shadow and cloud image and in the shadow area, which was found to be 0.305. A final output image is produced from the original defected pixel values except at identified shadow areas, where the reconstructed image was used. The results of one to four decomposition levels are demonstrated in Figure 5. A simple edge suppression algorithm that utilizes Gaussian filter wad applied to enhance the shadow area edges.

3.4 Results Evaluation and Discussion

Figure 5 shows the results obtained with different number of wavelet decomposition levels. Using two or three levels of decomposition gave the best visual results in terms of enhancing the high frequency component in the shadow areas. This is shown in the marked runway and road areas. Less detail were shown in the shadow areas if single decomposition level is used. On the other hand, using four levels of wavelet decomposition led to significant increase in the introduced artifacts in the output image. Figure 5 also shows that although shadow areas were significantly enhanced, these areas look patchy due to edge problems. Edge problems are mainly the result of the limitation of the shadow detection algorithm. Enhancement of cloud and shadow detection procedures should lead to significant reduction of this problem effect.

In order to quantify the obtained results two metrics were used. The first metric is the RMSE computed for the difference between each output image and the reference cloud-free image shown in figure 4 above. The second used metric is the entropy computed for each output image, the original image, and the reference image. Table 1, which summarizes the computed metrics, shows that the RMSE computed for the images resulting from applying the developed algorithm is less than the value computed for the original image, which indicates enhancement in image quality regardless of the number of used wavelet levels. The RMSE values for the output image obtained using 2 wavelet decomposition levels gave the least value of the RMSE. The high value of computed RMSE for all images could be attributed to the clouds existence in the output and original images compared to the cloud-free reference image.

Table 1 shows an increase in the computed entropy values with the increase in the number of wavelet decomposition levels. This might be attributed to the increase in the added details due to the increase in coefficient values at more wavelet levels. It should be noticed here that the increase in the entropy value does not indicate enhancement in the image. This is clear for the output image that resulted from applying the developed algorithm on four decomposition levels. The entropy value for this image is large while the image suffers many unwanted artifacts. Generally, the entropy values for the output image are higher than the entropy for the original image. Again the consistence difference between the reference and output images entropy may be attributed to the cloud existence in the latter images.

No of wavelet levels	RMSE	Entropy
1	48.1074	6.0483
2	48.0001	6.0886
3	48.0757	6.0954
4	47.8091	6.0959
Original Image	52.9923	6.0759
Reference Image		6.9761

Table 1. RMSE and entropy computed for output, original and reference images

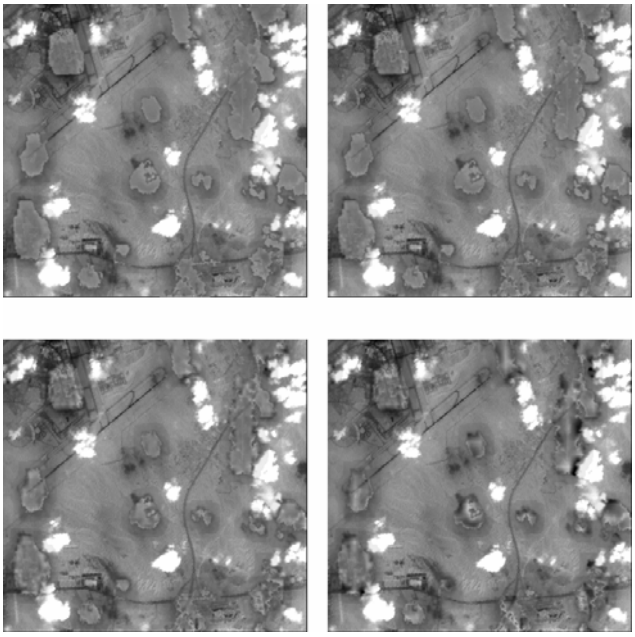

Figure 5. Output enhanced image using different wavelet decomposition levels: single level (top-left), two levels (top-right), three levels (bottom-left), and four levels (bottom-right)

4. CONCLUSION

A new algorithm for enhancing cloudy images by eliminating cloud-related shadows was developed and tested. The developed algorithm was successful in eliminating shadows from a single cloudy image while preserving underneath details. The algorithm adjusts the high frequency content in shadow areas by boosting the image wavelet coefficients before final image reconstruction. Several discrete wavelet decomposition levels were tested. The increase in image wavelet coefficient was determined by inspecting the image entropy in the shadow and the rest of the image. Visual and quantitative analysis of the results revealed that the ability to enhance details under shadow areas increased with the increase in the number of wavelet decomposition levels. Nevertheless, the higher this level is, the more artifacts in the output image. Generally, two or three wavelet decomposition levels were found to be sufficient for the analysis used in this study.

The obtained results, although revealed under shadow details, were patchy. One of the factors causing the patchy appearance of the shadow areas is the errors in the used shadow detection algorithm. Finally, it should be mentioned here that although the developed algorithm was tested on cloud-related shadows, it is believed that this algorithm can be implemented on large patches of shadows casted by features other than clouds given that the appropriate shadow detection algorithm is applied.

5. REFERENCES

Abd-Elwahab, M. A.,2006. *Image Fusion Techniques and Its Applications in Mapping*. Ph.D. Thesis, Faculty of Engineering, Ain Shams University, Cairo, Egypt.

Barkener, K.,2002. *Enhancement of scanned documents in Besov spaces using wavelet domain representations*. Proceedings of SPIE Vol. 4670

Berbar, M.A.; Gaber, S.F.,2004. *Clouds and shadows detection and removing from remote sensing images*, Electrical, Electronic and Computer Engineering, ICEEC '04', 2004 International Conference, 5-7 Sept. 2004, pp. 75-79.

Belward, A.S. and Valenzuela, C.R.,1991. *Remote Sensing and Geographic Information Systems for Resource Management in Developing Countries*, Kluwer Academic Publishers, London.

Bouyahia, S.; Mbainaibeye, J., and Ellouze, N.,2004. *Computer-aided diagnosis of mammographic images. Control*, Communications and Signal Processing, 2004. First International Symposium, pp. 259-262, 2004

Burrus, C. S. and R. A. Gopinath, H. Guo. *Introduction to Wavelet and Wavelet Transforms*, A Primer. Upper Saddle River, NJ (USA): Prentice Hall,1998.

Donoho, D.L.,1995. *De-noising by soft-thresholding*, IEEE Trans. on Inf. Theory, 41, 3, pp. 613–627.

Haralick, R. and Shapiro, L.,1992. *Computer and Robot Vision*, Addison-Wesley Publishing Company, NewYork.

Shaker, I., Abd-Elrahman, A., Abdel-Gawad, A., Abdelwahab, M. A.,2005. *Toward Removing Cloud and Shadow Effects in Satellite Images Using Image Fusion Techniques*. The Scientific Engineering Bulletin, Faculty of Engineering, Ain Shams University, Cairo, Egypt, 40(2):112-117.

Simpson, J.J. and Stitt, J.R.,1998. *A Procedure for the Detection and Removal of Cloud Shadow from AVHRR Data over Land*. IEEE Transactions on Geoscience and Remote Sensing, Vol. 36, No 3, May 1998 pp.880-897.

Wang, B. and Ono, A., 1999. *Automated Detection and Removal of Clouds and Their Shadows from Landsat TM Images*. IECE Transactions Inf.& Syst., (E82-D)2:453-460.

Finlayson, G.D, Hordley, S.D. and Drew, M.S,2002. *Removing Shadows from Images*. *In Proc. of European Conf. on Computer Vision,* Vol.4, pp. 823.836, 2002

Marini, D. and Rizzi, A.,2000. *A computational approach to color adaptation effects,* Image and Vision Computing, 18(13):1005-1014.

Zhou, G., Qin, Z., Benjamin, S., and Schickler, W.,2003. *Technical Problems of Deploying National Urban Large-scale True Orthoimage Generation*. The 2nd Digital Government Conference, Boston, May 18-21,2003, pp. 383-387